Clinical Cancer Investigation Journal-ISSN: 2278-0513

The Effect of TLCD and TMD[1] on Floating Breakwaters Against Waves

Short Title: TLCD and MDS in floating Breakwater

Abstract

Four different models of floating breakwaters were investigated and numerically simulated in this study, all of which had mass and liquid column dampers. All elements of solid type were modeled in Abacus software "concrete, water, soil, damper, breakwater". The type of analysis is dynamic and explicit, and the nonlinear effects of deformation are considered. This study compares different dampers with the damping of waves and seismic forces. The originality of this method is related to comparing the numerical results of a simulated model in Abacus and comparing it with the laboratory results of the same approved model and examining the different models and the results of the diagrams drawn from them, we conclude that if we use TLCD liquid column and TMD mass dampers as hybrids on the floating breakwater used in this paper, the greatest reduction effect on displacement and slip variables will be created for us. And the finite element method has been used for meshing different components for dynamic analysis. This article aims to obtain an optimal composition to minimize slippage and displacement in the floating breakwater article.

Keywords: *Floating breakwater, Numerical analysis, Wave impact, Earthquake impact*

Armin Behrooyan[1*], Mohammad Asadian Ghahfarrokhi

[1]*Master of Civil Engineering in Marine Structures, Science and Research, Islamic Azad university, Iran*

[2]*Assistant Professor of Civil Engineering in Marine Structures, Science and Research University of Tehran, Iran; asadian@srbiau.ac.ir*

**Corresponding author: armin.behrooyan@srbiau.ac.ir*

1. Introduction

Breakwaters are structures built to manage the harbor, ensure the safe entry of ships into waterways and ports [72-74], reduce the energy of waves, therefore, protecting beaches against the waves [22-26]. They offer advantages such as protection of access channels [88-90], protection of the coast and ports, protection against tsunami waves, and reduction of the energy of waves in seas and oceans [1, 27-30]. With the increased transportation of goods, the need for port development [84-87], and the increased size of vessels has necessitated the construction of breakwaters at greater depths and open places [31-35]. This has led to increased wave height and design and operation problems, leading to the investigation of various types of breakwaters in terms of structure and stability [36-40]. In terms of location, breakwaters can be divided into two categories: attached and detached [11-13, 66-68].

Floating breakwaters are constructed with the assumption that most wave energy is concentrated at the top [41-45]. These breakwaters are mostly temporary [47-51]. They can only be used to dampen low waves [14-16, 46]. The main shortcoming of floating breakwaters is that although they dampen some of the wave energy [79-83], their oscillation causes low waves because they oscillate along with the waves, which can be problematic [52-55]. Floating breakwaters can be made of various materials [17-20, 69-71].

Lee et al. [2] (2005) examined a typical tension from a floating platform with a Tuned Liquid Column Damper (TLCD). He aimed to find an economical mean of reducing vibrations caused by the floating wave system. In their 2008 study, Colul and Basso [3] stated that with the larger size of marine wind turbines, which are mostly forced out in the sea and are under more pressure from wave forces, the analysis of the dynamics to minimize the responses to these structures was necessary. In this study, the structural responses of offshore wind turbines with a connected damper (TLCD) are simulated. In a 2012 study, Lee and Jwang [4] used typical traction of the floating platform with a creative concept of an Underwater Tuned Liquid Column Damper (UWTLCD) alarm system. This study aimed to improve structural safety by reducing the oscillation and stress caused by waves in the submarine tension-leg platform (TLP). Mato et al. [5] (2014) stated that many researchers had considered passive oscillation control in recent years. Various types of devices have been proposed to reduce the dynamic response. Structural systems are very effective in reducing structural oscillations Tuned Liquid Column Damper (TLCD). In 2017, Christoph Adam et al. [6] presented a straightforward approach to the optimal design of a TLCD attached to a base-isolated structure. The function of the base-isolated structure well-appointed with the optimally tuned TLCD device compared to simple base structures was numerically and experimentally evaluated. Ming Chang et al. (2018) [7] stated that tuned mass dampers are widely accepted controlling methods for effective oscillation reduction. Christov et al. (2018) [8] stated that by coupling a float with a Tuned Liquid Multi-Column Damper (TLMCD), a structural damping device influenced by a Tuned Liquid Column

[1] **The Liquid Column and Mass Dampers**

Damper (TLCD) could be modeled using Lagrangian mechanics. The results indicate that the TLMCD used is better than the use of multiple TLCDs for this application. In their 2019 study, Joufi et al. [9] stated that Tuned Liquid Damper (TLD) and Tuned Liquid Column Damper (TLCD) are two kinds of passive control devices that are widely used in structural control.

Floating breakwaters can be installed, moved, and reused in various conditions, even in deep water [56-60]. Nevertheless, their complex dynamic response to the wave transfer makes them suitable only for a given period [61-65]. In this study, using the hydrodynamics of non-compressible smooth particles with a three-stage algorithm, the effects of waves on a couple of floating breakwaters and the combinations of the floating breakwaters have been investigated. So far, little to no studies have been performed on the use of TLCD in the marine industry, and mostly, the emphasis has been on the stability of platforms and jackets. In the marine industry, the TMD system has not been studied separately or in hybrid combinations. Therefore, the present study investigates the performance of liquid and mass column dampers in improving the oscillating behavior of floating breakwaters against waves. Overall, our purpose is to use TLCD and TMD dampers on a floating breakwater. The breakwater resistance using these dampers is against the waves and seismic forces and finding the optimal state. Therefore, this article achieves this main issue by using numerical modeling and studying the results.

1.1. Wavefield Description

The Persian Gulf is a large semi-enclosed sea at the northwestern end of the Indian Ocean. The JONSWAP spectrum was formulated for the developing state of the sea under enclosed conditions. The characteristics of the Persian Gulf are consistent with this basic assumption.

$$S(f) = \frac{\alpha g^2}{(2\pi)^4 f^5} \exp\left[-1.25\left(\frac{f}{f_p}\right)^{-4}\right] \gamma^{\exp\left(\frac{(f-fp)^2}{-2\sigma^2 f_p^2}\right)} \quad (1)$$

γ is the amplification factor of the peak, σ is the amplitude factor of the peak, g is the gravitational acceleration, f is the wave frequency, and f_p is the dominant spectral frequency. The JONSWAP project data were used to extract constant values of σ and α. In Eq. 3, H_s is a significant wave height.

$$\sigma = \begin{cases} 0.07 \text{ for } f < f_p \\ 0.09 \text{ for } f \geq f_p \end{cases}$$
$$\alpha = 4.5 \mathrm{H}_s 2 \mathrm{f}_\mathrm{p} 4 \quad (2)$$

The combination of multiaxial multipolar linear waves for the calculation of the horizontal and vertical velocities of water particles for random waves is as follows:

$$\mathrm{u}(\mathrm{x},\mathrm{z},\mathrm{t}) = \sum_{\mathrm{i}=1}^{\mathrm{n}} \mathrm{a_i} \cdot 2\pi \mathrm{f_i} \frac{\cosh(\mathrm{k_i}(z+\mathrm{h}))}{\sinh(\mathrm{k_i h})} \cos(k_i x - 2\pi f_i t + \varepsilon_i) \quad (3)$$

$$\mathrm{w}(\mathrm{x},\mathrm{z},\mathrm{t}) = \sum_{\mathrm{i}=1}^{\mathrm{n}} \mathrm{a_i} \cdot 2\pi \mathrm{f_i} \frac{\sinh(\mathrm{k_i}(\mathbf{z}+\mathrm{h}))}{\sinh(\mathrm{k_i h})} \sin(k_i x - 2\pi f_i t + \varepsilon_i) \quad (4)$$

1.2. Analysis of Hydrodynamic Forces

Hydrodynamic analysis of a floating breakwater exposed to irregular waves is performed to acquire a dynamic response from the floating body and the time history of tensile stress in mooring lines. Potential flow theory and the three-dimensional panel method were used to extract hydrodynamic loads. ANSYS AQWA uses a hybrid method to model large floating structures such as a floating breakwater. First-order potential flow theory is used for radiation and diffraction analysis. The hydrodynamic pressure distribution is estimated by the Bernoulli linear equation [10-11].

$$\mathrm{p}^{(1)} = -\rho \frac{\partial \varphi(\vec{\mathrm{x}},\mathrm{t})}{\partial \mathrm{t}} = \mathrm{i}\omega\rho\varphi(\vec{\mathrm{x}})\mathrm{e}^{-\mathrm{i}\omega t} \quad (5)$$

In Eq. 6, ρ is the density of seawater and ω is the angular frequency of the wave. The first-order hydrodynamic force on the floating body (vessel) is obtained as follows through the integration of dynamic pressure on the wet surface of the body, S0:

$$\mathrm{F_{Ij}} = -\mathrm{i}\omega\rho\left(\int \varphi_\mathrm{I}(\vec{\mathrm{x}})\mathrm{n_j}\mathrm{ds}\right)_{s_0} \quad (6)$$

$$\mathrm{F_{Dj}} = -\mathrm{i}\omega\rho\left(\int \varphi_\mathrm{D}(\vec{\mathrm{x}})\mathrm{n_j}\mathrm{ds}\right)_{s_0} \quad (7)$$

$$\mathrm{F_{Rjk}} = -\mathrm{i}\omega\rho\left(\int \varphi_{\mathrm{Rj}}(\vec{\mathrm{x}})\mathrm{n_j}\mathrm{ds}\right)_{s_0} \quad (8)$$

FIj is the incidental wave force, FDj is the scattered wave force, and FRjk is the radiated force caused by the unit motion range of the floating body wheel. In the above equations, φI is the first-order incidental wave potential with unit wave amplitude, φD is the equivalent scattered wave potential, and φRj is the radiated wave potential caused by the motion j of the floating body with unit motion range. To resolve these equations, the Hess-Smith panel method has been used. The average wet surface of the floating body is separated into quadrilateral plates. The potential and power of the source on each page are assumed to be constant. Therefore, the corresponding mean values at each panel level are obtained for simulation [10].

1.3. Mooring System Forces

The mooring system is investigated according to the interaction between the connecting lines and the movements of the floating body. Each connecting line is divided into several

Morrison elements. Fig. 1 indicates the related configuration. The response of the entire T-line is a compound of low-frequency TLF force and wave-frequency TW [5]:

T = TLF + TWF

(9)

The quasi-static method has been used to extract the low-frequency stress from the compensation of the floating body. For the zero-gradient connecting line at the anchor junction at the seabed, the connecting line responses in the local axis system are as follows [10]:

$$H_2 = AE\left(\sqrt{\left(\frac{T_2}{AE}+1\right)^2 - \frac{2wZ_2}{AE}} - 1\right) |$$

(10)

$$X_2 = H_2\left(\frac{1}{w}\sinh^{-1}\left(\frac{WL}{H_2}\right) + \frac{L}{AE}\right) \quad (11)$$

$$V_2 = wL \quad (12)$$

$$T_2 = \sqrt{H_2^2 + V_2^2} \quad (13)$$

It is the cross-sectional area of the connecting line, E is Young's modulus, L is the non-extended length of the connecting line, and w is the immersion weight per unit length. As indicated in Fig. 1, the local x-axis is an anticipation of the vector that joins the anchor point and the fair lead in the bed, and it shows vertical z-axis points.

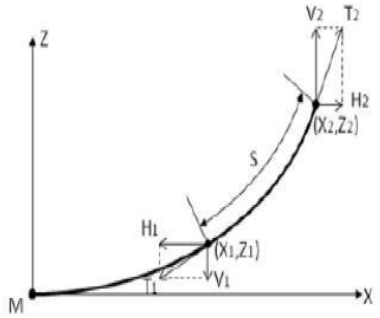

Figure 1: Geometry of connecting lines [5]

The values obtained for the external and momentary forces of action at the center of gravity of the floating body are considered. The following geometric coefficient has been used in mines.

$$\bar{k} = \frac{2h}{3L_1}\left(1 + \frac{3L^2}{4h^2} + \frac{A_h}{A_v}\frac{L^3}{8h^3}\right)$$

(23)

1.4. TLCD Equations

Retire and Ziegler (2006) obtained the equation of fluid motion inside the horizontal and vertical columns using the modified Bernoulli equation along the non-pressurized flow line [10]:

$$\ddot{U} + \delta_L|\dot{U}|U + \omega_A^2\left[1 - k_1\frac{a_{z'}}{H\omega_A^2} - k_2\frac{\dot{v}^2}{\omega_A^2}\right]U = k\left[a_{y'} - g\vartheta\right] - k_1\frac{B}{2}\ddot{\theta} \quad (14)$$

δL is the apex descent coefficient, and ωA is the non-circular natural frequency TLCD. The geometric coefficients used in the equation are as follows:

$$k_1 = \frac{2h}{L_{eff}} \quad (15)$$

$$k_2 = \frac{L+2h}{L_{eff}} \quad (16)$$

$$k = \frac{L}{L_{eff}} \quad (17)$$

$$L_{eff} = 2h + \frac{A_v}{A_h}L \quad (18)$$

h is the length of the liquid column in the vertical section of the tube at rest, L is the horizontal length of the liquid column, Av is the vertical cross-sectional area of the liquid column, and Ah is the horizontal cross-section of the liquid column. The liquid column's absolute acceleration of TLCD at the reference point of A (z', y') is as follows [10]:

$$\overrightarrow{a_A} = \ddot{v}\overrightarrow{e_y} + \ddot{\omega}\overrightarrow{e_z} - dA\left(\ddot{\vartheta}\overrightarrow{e_{y'}} + \dot{\vartheta}^2\overrightarrow{e_{z'}}\right) \quad (19)$$

$\ddot{v}$, $\ddot{\omega}$, and $\ddot{\vartheta}$ are the impeccable translational and rotational accelerations of the main structure around its center of gravity. With a normal incidental wave, the damping device's response to the motion of the floating breakwater is shown by two vertical forces at any moment. These effective parameters are applied to an imaginary TCLD reference point. Using the motion retention principle and if the point of application is transferred from the reference point to the center of gravity of the floating body, the reaction and momentary force transmitted from the damper to the floating breakwater is as follows [10]:

$$F_{y'} = m_f\left[a_{y'} - \frac{L}{L_1}\left(u - u\dot{\vartheta}^2\right) + \frac{1}{L_1}\left((h^2+u^2)\ddot{\theta} + 4uuu\dot{\theta}\right)\right] \quad (20)$$

$$F'_z = m_f\left[a_{z'} - \frac{L}{L_1}\left(u\ddot{\theta} + 2u\dot{\theta}\right) + \frac{1}{L_1}\left((h^2+u^2)\dot{\theta}^2 - 2(\dot{u}^2 + uui)\right]\right. \quad (21)$$

$$M_{Ax} = m_f\left\{-a_{y'}d + \frac{1}{L_1}\left[\right. Lhi\ - 4\,uu\,\dot{\theta}d + (h^2+u^2)\left[a_{y'} + g\vartheta - d\ddot{\theta}\right]\right] + \frac{2h}{L_1}\left[u^2\ddot{\theta} + 2uu\dot{\theta}\right] + \bar{k}h^2\ddot{\theta}\right\} \quad (22)$$

1.5. TMD DAMPER

The demonstration of tuned mass damper performance is shown in Figure 2.

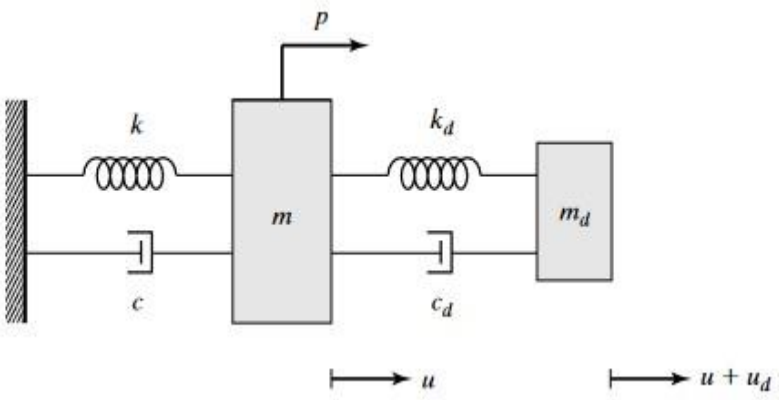

Figure 2: The Concept of the Tuned Mass Damper [21]

Tuned mass $\ddot{u}_d + 2\xi_d\omega_d\dot{u}_d + \omega_d^2 u_d = -\ddot{u}$ (24)

The purpose of adding the mass damper is to cap the motion of the structure when subjected to a particular excitation. The design of the mass damper involves specifying the mass MD, stiffness KD, and damping coefficient CD. The optimal choice of these quantities is discussed in the following section. In this example, the near-optimal approximation for the frequency of the damper,

$$\omega_d = \omega \qquad (25)$$

$$u = \hat{u}\sin(\Omega t + \delta_1)$$
$$u_d = \hat{u}_d \sin(\Omega t + \delta_1 + \delta_2)$$

U and δ denote the displacement amplitude and phase shift; respectively, the critical loading scenario is the resonant condition, **Ω** = ω. The solution for this case has the following

$$\hat{u} = \frac{\hat{p}}{km}\sqrt{\frac{1}{1+\left(\frac{2\xi}{\bar{m}}+\frac{1}{2\xi_d}\right)^2}} \qquad (30)$$

$$\hat{u}_d = \frac{1}{2\xi_d}\hat{u} \qquad (31)$$

$$\tan\,\delta_1 = -\left[\frac{2\xi}{\bar{m}} + \frac{1}{2\xi_d}\right] \qquad (32)$$

$$\tan\,\delta_2 = -\frac{\pi}{2} \qquad (33)$$

In this study, the displacement values are applied to the end of the longitudinal reinforcing elements for loading in the form of displacement. The loads applied to the structure are the forces exerted due to the applied earthquakes and the waves and winds.

In this study, four models of floating breakwaters have been studied and numerically simulated. The first model simulates the floating breakwater under impact waves with a wave breaking height of 6.3 m, a period of 15.4 s, and the perceived earthquake. The second model assumes that the breaking

is used to show the design procedure. The stiffness for this frequency combination is correlated by:

$$k_d = \bar{m}k \qquad (26)$$

corresponds to tuning the damper to the fundamental period of the structure. Considering a periodic excitation**,**

$$p = \hat{p}\sin\,\Omega t \qquad (27)$$

the answer is given by:

(28)

(29)

form:

height of impact waves is 9.2 meters with a period of 18.6 s. In the third model, the breakwater has been simulated in a calm sea without wave impact and only under the influence of the earthquake. In the fourth model, floating breakwaters are modeled only under impact waves with a wave breaking height of 6.3 m and without the influence of earthquakes on breakwaters. To consider the earthquake's impact on the structure, the data related to horizontal seismic drift are introduced in the seismic loading section of the software. Fig 4 Table 1 shows the models used in the present study.

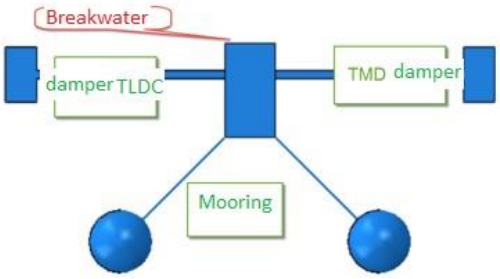

Figure 3: Wave Breaker Cross-section along with Mooring and Damper

The diameter and length of the moorings used in this analysis are 15 cm and 18.5 cm, respectively (Fig. 3).

Table 1: Study Samples

Earthquake	Model	Wave breaking height $H_{(S)}$	$T_{(S)}$	Wave direction
Yes	1	6.3	5.53	Normal
Yes	2	9.2	6.38	Normal
Yes	3	----	…	Normal
No	4	6.3	5.61	Normal

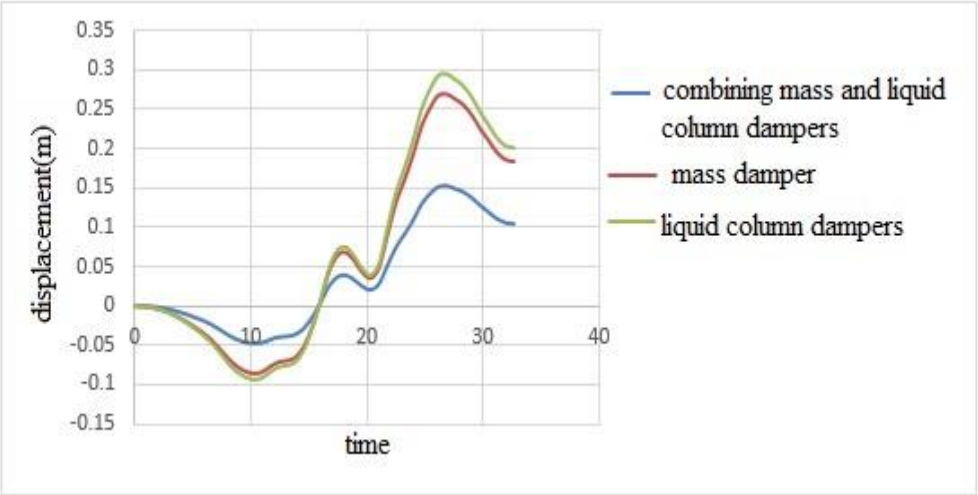

Figure 4. Displacement of Sample 1

1.6. Palmgren-Miner Law

According to Palmgren-Miner law, the accumulative fatigue damage is obtained as follows:

$$D = \sum \frac{n_i}{N_{ti}} \quad (34)$$

D is the accumulated fatigue damage, ni is the number of stress cycles in the i^{th} stress block, and Nti is the number of failure cycles under the constant stress area Δσ. The fatigue lifecycle is opposite the accumulated fatigue damage.

$$L_{Fatigue} = \frac{1}{D} \quad (35)$$

FLS has been considered to ensure that any component in the connecting line has adequate resistance to a malfunction caused by fatigue. Based on the DNVGL-OS-E301 recommendation, the FLS design equation is as follows [10]:

$$1 - D \cdot \gamma_f \geq 0 \quad (36)$$

2. Materials and Methods

2.1. Study Validation

The two-dimensional geometric model studied in the present study consists of a pair of floating breakwaters, a coastal wall, and a sine wave generating wall modeled in Abacus. The floating breakwater couple consists of two bodies with a hollow square cross-section with dimensions of 52x52 m and an immersion height of 3 m. The right-hand wall represents the coastal wall, and the left-hand wall produces the sea wave. The floating-submersible hybrid breakwater is also investigated by adding a trapezoidal submersible breakwater height of 0.8 m and a slope angle of 45° to the model mentioned above of the floating breakwater couple. As mass and spring systems, floating breakwaters equalized 50 N/m cables in Abacus. Fig. 5

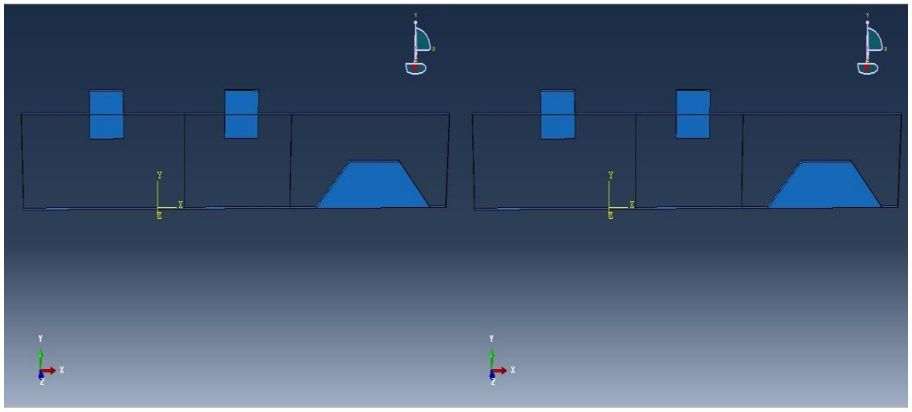

Figure 5: Model Used for Study Validation

2.2. Materials

We used concrete, soil, water, steel, and materials to model different models in Abacus software. The specifications of the materials used are given in the table below.

Table 2- Materials to Model Different Models in Abacus Software

NAME MATERIALS	MASS DENSITY	YOUNG MODULUS	POISSON RATIO	YIELD STRESS	PLASTIC STRAIN
WATER	1000	3.1E06	-	-	-
SOIL	1800	20000000	0.2	-	-
CONCRETE	2400	20000000000	0.2	75000000	0
STEEL	7850	20000000000	0.3	400000000	0

3. Results

3.1. Model 1

It is assumed in this model that the floating breakwater under study is affected by the simultaneous loading of the wave and the earthquake. The wave force is applied to the breakwater by the impact of a wave with a breaking height of 6.3 m, and the earthquake is shown according to the drift pattern. The following figures 6 and 7, show the simulation results regarding displacement of the studied breakwater in the x and y directions for Model 1.

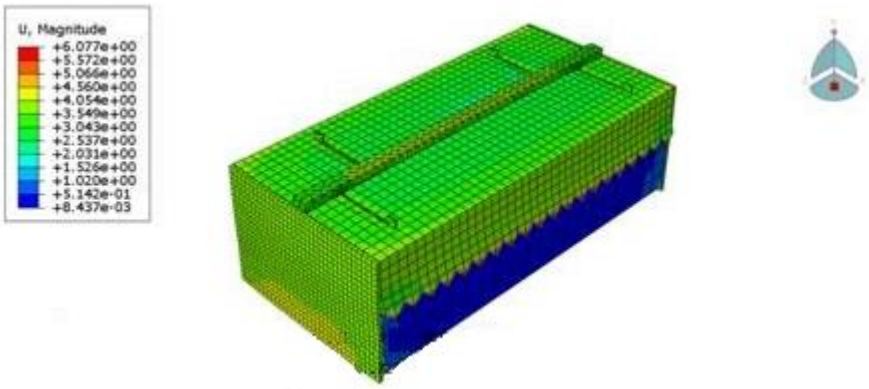

R2019xODB: Job-4.odb Abacus/Expt DEY M Jan 22 19-40:38 Iran standard Time 2021 Step: Step-1 Increment 23007: Step Time = 0.0728 Primary Var: U, Hagnitude

Figure 6. Displacement contour for sample No. 1

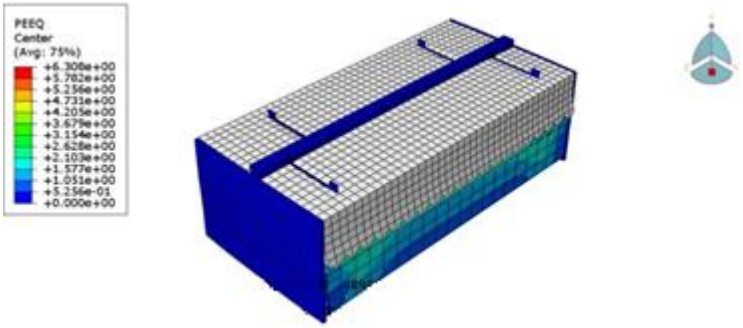

ODB: Job-4.odb Abacus/Exp DEPERIeNeE R2019x Fri Jan 22 19:40:38 Iran Standard Time 202:1 Step: Step-1 Increment 23807: Step Time = 0.0128 Primary Var: PEEQ

Figure 7: Bearing Stress Contour between the Breakwater and the Soil Bed of Sample 1

3.2. Model 2

In this model, it is assumed that the wave enters the breakwater with a breaking height of 2.9 m. It is also assumed that the breakwater is simultaneously affected by the earthquake. The software ran with the mentioned conditions, and the following Figures 8, 9, 10, and 11, were obtained.

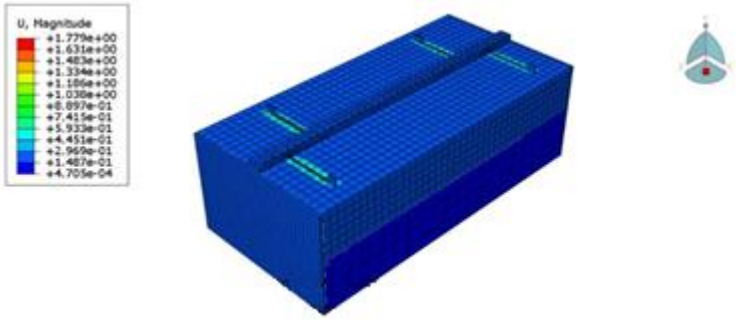

ODB: Job-4.odb Abacus/Explco ER2019×Fri Jan 22 19:40:38 Iran Standard Time 2021 Step: Step-1 Increment 5951 : Step Time = 0.2 Primary Var: U, Magnitude

Figure 8: Displacement Contours in Sample 2

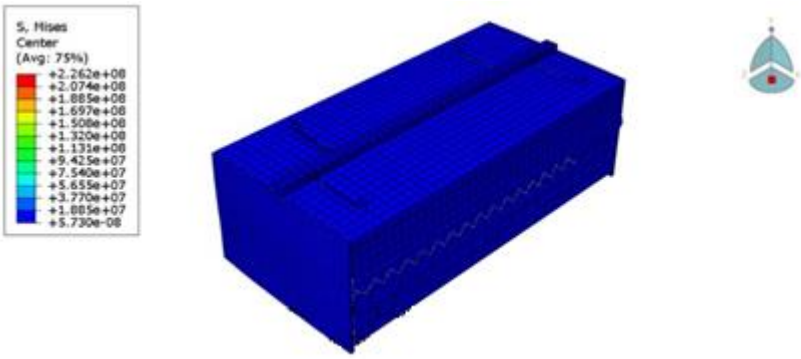

ODB: Job-4.odb Abacus/Exp ER2019x Fri Jan 22 19:40:38 Iran Standard Time 2021 Step: Step-1 Increment 23807: Step Time =0.8128Primary Var: S, Mises

Figure 9: Von Mises Stress Contours in Sample 2

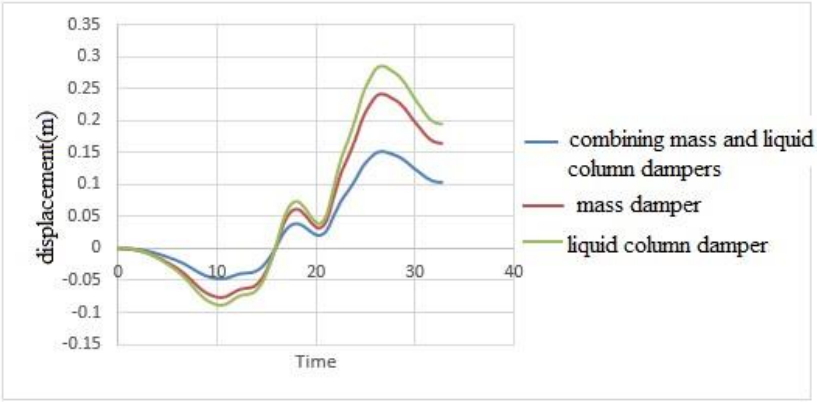

Figure 10: Displacement of Sample 2

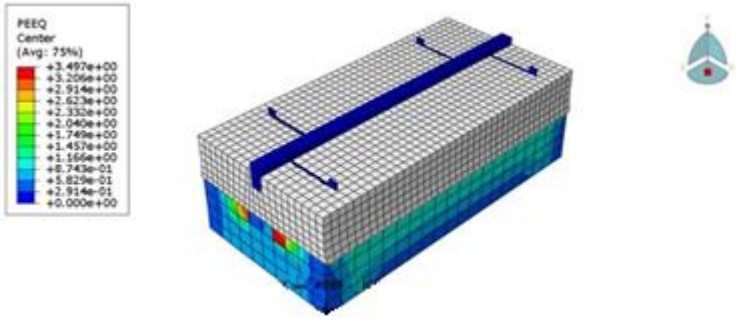

ODB: Job-4.0db Abaqus/Explict 3DEXBERIENCE R2019x Fri Jan 22 19:40:38 Iran Standard Time 2021Step: Step-1 Increment 17855: Step Time = 0.6916 Primary Var: PEEQ

Figure 11: Variations of Stress at the Breakwater Leg (Pascal) Model 2

3.3. Model 3

In this model, the floating breakwater studied is only affected by the earthquake load, and it is assumed that no waves enter the breakwater. This model investigates and obtains the percentage change of stresses and breakwater displacements studied in different scenarios. Figs. 12, 13, 14, and 15

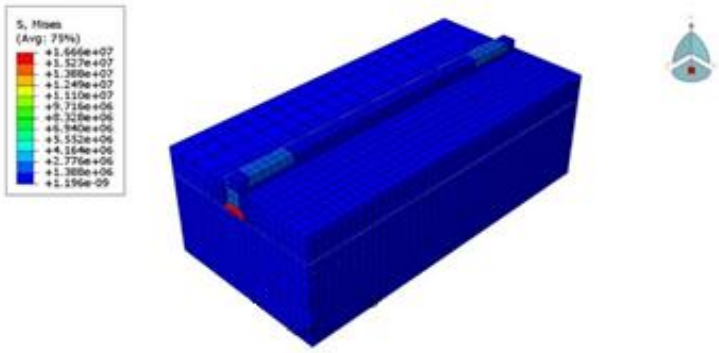

ODB: tanctrg.odb Abag R2019x Sun May 24 23:33:16 Iran Daylight Time 2020 Step: Step-1 Increment 678: Step Time = 0.8128 Primary Var: S, Mises

Figure 12: Stress Variation Contours of the Studied System (Pascal) for Model 3

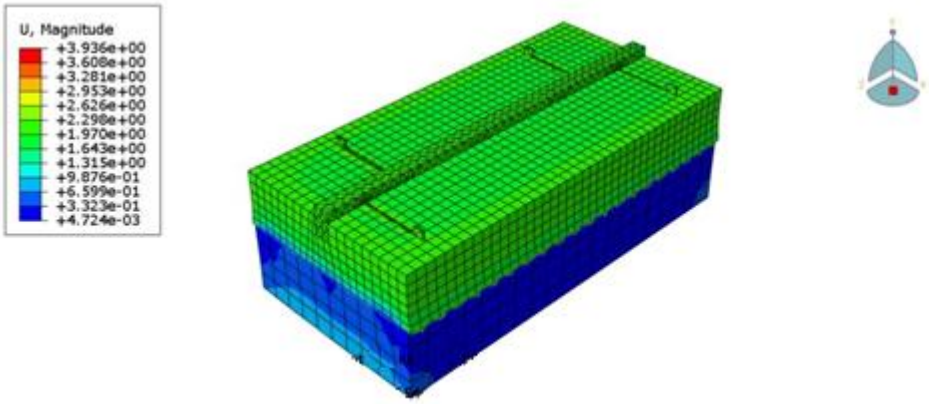

ODB: Job-4.odb Abacus/Explic R2019x Fri Jan 22 19:40:38 Iran Standard Time 2021 Step: Step-1 Increment 17855: Step Time = 0.6546 Primary Var: U, Magnitude

Figure 13: Displacement Contours (Meters) in the x-direction for Model 4

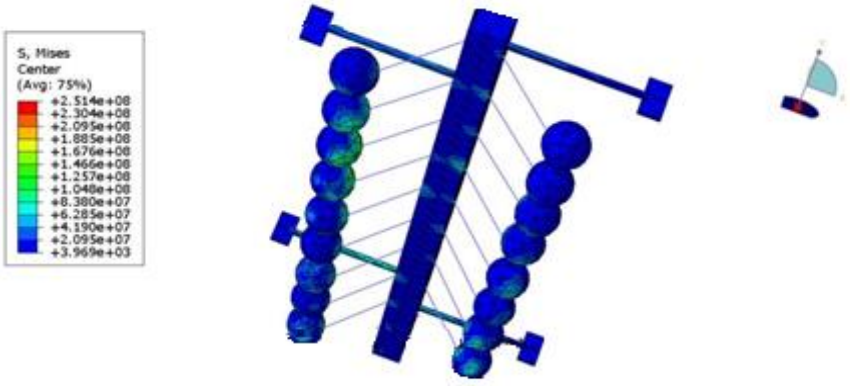

ODB: Job-4.odb Abaqus/ Explic R2019x 19:40:38 Iran Standard Time 2021 Step: Step-1 Increment 33719: Step Time=1.236 Primary Var: S, Mises

Figure 14: Stress Variations in Breakwater and Mooring (Pascal) for Model 2

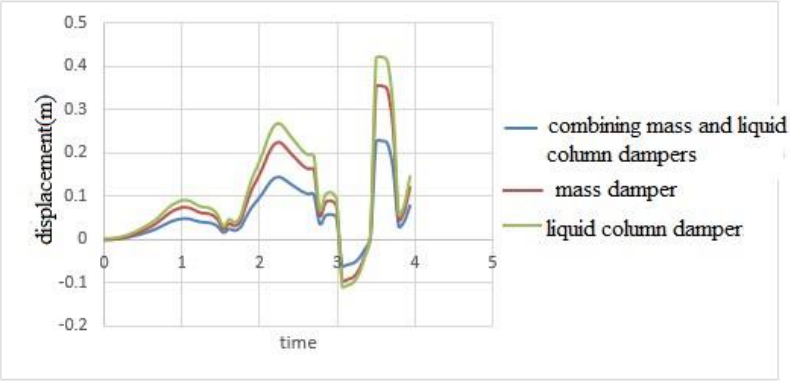

Figure 15: Maximum Displacement in Sample 3

3.4. Model 4

In model 4, the breakwater is assumed to be only affected by a wave with a breaking height of 6.3 m, and the seismic force is ignored. The results obtained from this model are shown in figures 16 and 17.

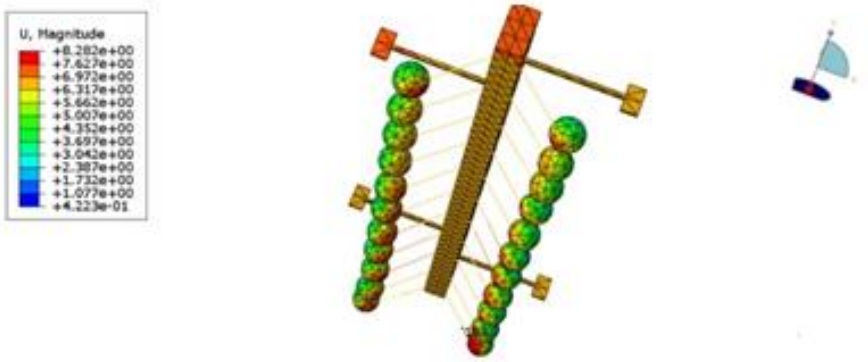

ODB: Job-4.odb Abacus/Explicit 3DEXPERIENCE R2015 Fri Jan 22 19:40:38 Iran Standard Time 2021 Step: Step-1 Increment 33719: Step Time =1.236 Primary Var: U, Magnitude

Figure 16: Displacement Contours in Breakwater and Mooring (Pascal) for Model 3

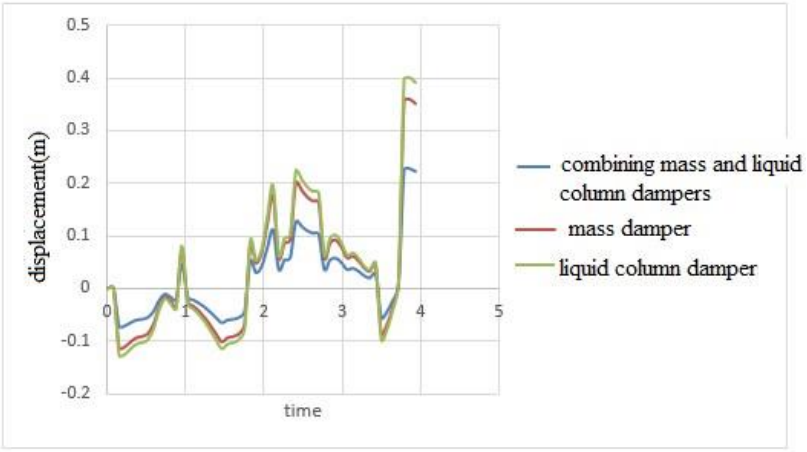

Figure 17: Maximum Displacement of Sample 4

4. Discussion

Table 3: Apex Displacement and Breakwater Slip in the Models of the Study (m)

Model	Breaking wave height (m)	Earthquake	Slip with liquid column damper	Slip with a mass damper	Slip with mass and liquid column dampers	Apex displacement with a mass damper	Apex displacement with the liquid column damper	Apex displacement with mass and liquid column dampers
1	6.3	Yes	0.040482	0.043408	0.02926	5.274541	4.606875	2.6325
2	9.2	Yes	0.036867	0.050705	0.038382	5.274542	5.955128	3.40293
3	Non-existent	----	0.028591	0.015819	0.012274	3.661937	4.134445	2.36254
4	6.3	No	0.023248	0.018141	0.018926	3.730742	4.212127	2.40693

In model 1- slip and displacement of mass dampers and liquid columns- their combination has created less displacement, and in model 1, the breaking height of the wave is considered 6.3m. Here there is also seismic force. In model 2, the liquid column damper has caused less slip than the mass damper combined with the liquid column. And in the displacement of the head, their combination has less displacement. In model 2, the breaking height of the wave is considered as 9.2 m. There is also a seismic force. In model 3, the combination of mass dampers and liquid columns creates less slip and displacement than all others. In model 4, the mass damper has less slip than the other three dampers combination, but in the displacement of the head, the combination of the mass damper and the liquid column gives it less displacement

5. Conclusion

In future research, the effects of using "TLCD and TMD," dampers, that have been looked into in this study, can be investigated on other breakwaters or even fixed breakwaters and platforms.

In general, the head displacement always gives us less displacement in all models, so the combination of mass damper and liquid column can be considered the optimal state. So, in general, according to the modeling and research, it can be considered that the combination of TLCD and TMD dampers on floating breakwaters gives us less displacement and damage caused by the seismic and waves forces. The performance of liquid and mass column dampers in improving the oscillating behavior of floating breakwaters against waves was investigated in this study. Using ANSIS Abacus, the performance of TLCD and TMD dampers was examined in separate (in the form of a table) and hybrid (in the form of a model and a table) manners. The geometry of the breakwater section is following Fig. (3). The software employed in this study is ABAQUS 2019.

Conflict of interest: None

Financial support: Self-funded

Ethical stataements: No

References

1. Seyed Yaghoub Zolfaghari Far, F.T., *A review of the history of breakwaters and their different types*, 2016

2. Lee, H., S.-H. Wong, and R.-S. Lee, *Response mitigation on the offshore floating platform system with tuned liquid column damper.* Ocean engineering, 2006. **33**(8-9): p. 1118-1142.

3. Colwell, S. and B. Basu, *Tuned liquid column dampers in offshore wind turbines for structural control.* Engineering Structures, 2009. **31**(2): p. 358-.368

4. Lee, H.H. and H. Juang, *Experimental study on the vibration mitigation of offshore tension leg platform system with UWTLCD.* Smart Structures and Systems, 2012. **9**(1): p. 71-104.

5. Di Matteo, A., et al., *Direct evaluation of the equivalent linear damping for TLCD systems in random vibration for pre-design purposes.* International Journal of Nonlinear Mechanics, 2014. **63**: p. 19-30.

6. Adam, C., et al., *earthquake excited base-isolated structures protected by tuned liquid column dampers: design approach and experimental verification.* Procedia Engineering, 2017. **199**: p. 1574-1579.

7. Chang, C.-M., S. Shia, and Y.-A. Lai, *Seismic design of passive tuned mass damper parameters using active control algorithm.* Journal of Sound and Vibration, 2018. **426**: p. 150-165.

8. Coudurier, C., O. Lepreux, and N. Petit, *Modelling of a tuned liquid multi-column damper. Application to floating wind turbine for improved robustness against wave incidence.* Ocean Engineering, 2018. **165**: p. 277-292.

9. Fei, Z., et al., a *Control performance comparison between the tuned liquid damper and tuned liquid column damper using real-time hybrid simulation.* Earthquake Engineering and Engineering Vibration, 2019. **18**(3): p. 695-701.

10. Shahrabi, M. and K. Bargi, *Enhancement the Fatigue Life of Floating Breakwater Mooring System Using Tuned Liquid Column Damper*. Latin American Journal of Solids and Structures, 2019. **16**(7).

11. Kalantari, S. S., & Taleizadeh, A. A. (2020). Mathematical modeling for determining the replenishment policy for deteriorating items in an EPQ model with multiple shipments.

International Journal of Systems Science: Operations & Logistics, 7(2), 164-171.

12. Wang, X., & Lyu, X. (2021). Experimental study on vertical water entry of twin spheres side-by-side. Ocean Engineering, 221, 108508. DOI: 10.1016/j.oceaneng.2020.108508.

13. Li, X., Yang, H., Zhang, J., Qian, G., Yu, H. Cai, J. (2021). Time-Domain Analysis of Tamper Displacement during Dynamic Compaction Based on Automatic Control. Coatings, 11(9). DOI: 10.3390/coatings11091092.

14. Samireh Kadaei, Seyedeh Mahsa Shayesteh Sadeghian, Marziyeh Majidi, Qumars Asaee, Hassan Hosseini Mehr, "Hotel Construction Management considering Sustainability Architecture and Environmental Issues," Shock and Vibration, vol. 2021, Article ID 6363571, 13 pages, 2021. https://doi.org/10.1155/2021/6363571.

15. Zhang, C., & Ali, A. (2021). The advancement of seismic isolation and energy dissipation mechanisms based on friction. Soil dynamics and earthquake engineering (1984), 146, 106746. DOI: 10.1016/j.soildyn.2021.106746.

16. Zhang, B., Chen, Y., Wang, Z., Li, J., & Ji, H. (2021). Influence of Mach Number of Main Flow on Film Cooling Characteristics under Supersonic Condition. Symmetry (Basel), 13(127), 127. DOI: 10.3390/sym13010127.

17. Bathaei, B. (2020). The Architectural System of Persian Enclosed Garden: Recognition & Recreating of the Concept of Persian Garden. LAP LAMBERT Academic Publishing.

18. Bathaei, B. (2018). Achieving Sustainable City by the Concept of Persian Garden. Acta Technica Napocensis: Civil Engineering & Architecture, 61(3), Special Issue– International Conference- Architecture Technology and the City Workshop Questions.https://constructii.utcluj.ro/ActaCivilEng/download/special/2018-10/ATN2018(3)_6.pdf

19. Bathaei, B. (2016). Change Is of the Essence, Regenerating of Brown Fields (Landscape Revitalization of Tehran's Brick Kilns). 2nd International Conference on Architecture, Structure and Civil Engineering (ICASCE'16), UK, London.

20. Hossein Eskandani, O., Doraj, P., 2021. Redevelopment of Brownfields, an Approach toward Sustainable Local Development. Turkish Journal of Computer and Mathematics Education (TURCOMAT), Research Article, Vol. 12, No. 13, 4808-4815.

21. ConCh04v2.fm Page 217 Thursday, July 11, 2002 4:33 PM

22. Hussain, N., Khan, M.A., Kadry, S., Tariq, U., Mostafa, R.R., Choi, J.I. and Nam, Y., Intelligent Deep Learning and Improved Whale Optimization Algorithm Based Framework for Object Recognition, 2021.

23. Lee, S. and Park, D., Adaptive ECGSignal Compression Method Based on Look-Ahead Linear Approximation for Ultra Long-Term Operating of Healthcare IoT Devices. 2021.

24. Lee, C.H. and Park, J.S., 2021. An SDN-Based Packet Scheduling Scheme for Transmitting Emergency Data in Mobile Edge Computing Environments. HUMAN-CENTRIC COMPUTING AND INFORMATION SCIENCES, 11.2021.

25. Baek, S., Jeon, J., Jeong, B. and Jeong, Y.S., 2021. Two-Stage Hybrid Malware Detection Using Deep Learning. HUMAN-CENTRIC COMPUTING AND INFORMATION SCIENCES, 11. 2021.

26. Dai, H., Li, J., Kuang, Y., Liao, J., Zhang, Q. and Kang, Y., 2021. Multiscale Fuzzy Entropy and PSO-SVM Based Fault Diagnoses for Airborne Fuel Pumps. Human-centric Computing and Information Sciences, 11. 2021.

27. Zhang, D., Chen, X., Li, F., Sangaiah, A.K. and Ding, X., 2020. Seam-carved image tampering detection based on the co-occurrence of adjacent lbps. Security and Communication Networks, 2020.

28. Song, Y., Zhang, D., Tang, Q., Tang, S. and Yang, K., 2020. Local and nonlocal constraints for compressed sensing video and multi-view image recovery. Neurocomputing, 406, pp.34-48.

29. Zhou, S. and Qiu, J., 2021. Enhanced SSD with interactive multi-scale attention features for object detection. Multimedia Tools and Applications, 80(8), pp.11539-11556.

30. Tang, Q., Wang, K., Yang, K. and Luo, Y.S., 2020. Congestion-balanced and welfare-maximized charging strategies for electric vehicles. IEEE Transactions on Parallel and Distributed Systems, 31(12), pp.2882-2895.

31. Wang, J., Chen, W., Ren, Y., Alfarraj, O. and Wang, L., 2020. Blockchain-Based Data Storage Mechanism in Cyber-Physical System. Journal of Internet Technology, 21(6), pp.1681-1689.

32. Song, Y., Li, J., Chen, X., Zhang, D., Tang, Q. and Yang, K., 2020. An efficient tensor completion method via truncated nuclear norm. Journal of Visual Communication and Image Representation, 70, p.102791.

33. Wang, J., Wu, W., Liao, Z., Jung, Y.W. and Kim, J.U., 2020. An Enhanced PROMOT Algorithm with D2D and Robust for Mobile Edge Computing. Journal of Internet Technology, 21(5), pp.1437-1445.

34. Zhang, D., Wang, S., Li, F., Tian, S., Wang, J., Ding, X., and Gong, R., 2020. An Efficient ECG Denoising Method Based on Empirical Mode Decomposition, Sample Entropy, and Improved Threshold Function. Wireless Communications and Mobile Computing, 2020.

35. Tang, Q., Wang, K., Song, Y., Li, F. and Park, J.H., 2019. Waiting time minimized charging and discharging strategy based on mobile edge computing supported by the software-defined network. IEEE Internet of Things Journal, 7(7), pp.6088-6101.

36. Zhang, J., Yang, K., Xiang, L., Luo, Y., Xiong, B., and Tang, Q., 2013. A self-adaptive regression-based multivariate data compression scheme with error bound in wireless sensor networks. International Journal of Distributed Sensor Networks, 9(3), p.913497.

37. Zhang, J., Sun, J., Wang, J. and Yue, X.G., 2020. Visual object tracking based on residual network and cascaded correlation filters. Journal of Ambient Intelligence and Humanized Computing, pp.1-14.

38. Gu, K., Wang, Y. and Wen, S., 2017. Traceable Threshold Proxy Signature. Journal of Information Science & Engineering, 33(1).

39. Li, W., Ding, Y., Yang, Y., Sherratt, R.S., Park, J.H. and Wang, J., 2020. Parameterized algorithms of fundamental NP-hard problems: a survey. Human-Centric Computing and Information Sciences, 10(1), pp.1-24.

40. Gu, K., Yang, L., Wang, Y. and Wen, S., 2016. Traceable identity-based group signature. RAIRO-Theoretical Informatics and Applications, 50(3), pp.193-226.

41. Yin, B., Zhou, S., Lin, Y., Liu, Y., and Hu, Y., 2014. Efficient distributed skyline computation using dependency-based data partitioning. Journal of Systems and Software, 93, pp.69-83.

42. Long, M. and Xiao, X., 2018. Outage performance of double-relay cooperative transmission network with energy harvesting. Physical Communication, 29, pp.261-267.

43. Xu, Z., Liang, W., Li, K.C., Xu, J. and Jin, H., 2021. A blockchain-based roadside unit-assisted authentication and key agreement protocol for the internet of vehicles. Journal of Parallel and Distributed Computing, 149, pp.29-39.

44. Wang, W., Yang, Y., Li, J., Hu, Y., Luo, Y. and Wang, X., 2020. Woodland labeling in chenzhou, China, via a deep learning approach. International Journal of Computational Intelligence Systems, 13(1), pp.1393-1403.

45. Chubo Liu, Kenli Li, Keqin Li: A Game Approach to Multi-Servers Load Balancing with Load-Dependent Server Availability Consideration. IEEE Trans. Cloud Comput. 9(1): 1-13 (2021)

46. Chubo Liu, Kenli Li, Keqin Li, Rajkumar Buyya: A New Service Mechanism for Profit Optimizations of a Cloud Provider and Its Users. IEEE Trans. Cloud Comput. 9(1): 14-26 (2021)

47. Guoqing Xiao, Kenli Li, Yuedan Chen, Wangquan He, Albert Y. Zomaya, Tao Li: CASpMV: A Customized and Accelerative SpMV Framework for the Sunway TaihuLight. IEEE Trans. Parallel Distributed Syst. 32(1): 131-146 (2021)

48. Mingxing Duan, Kenli Li, Keqin Li, Qi Tian: A Novel Multi-task Tensor Correlation Neural Network for Facial Attribute Prediction. ACM Trans. Intell. Syst. Technol. 12(1): 3:1-3:22 (2021)

49. Cen Chen, Kenli Li, Sin G. Teo, Xiaofeng Zou, Keqin Li, Zeng Zeng: Citywide Traffic Flow Prediction Based on Multiple Gated Spatio-temporal Convolutional Neural Networks. ACM Trans. Knowl. Discov. Data 14(4): 42:1-42:23 (2020)

50. Xu Zhou, Kenli Li, ZhiBang Yang, Yunjun Gao, Keqin Li: Efficient Approaches to k Representative G-Skyline Queries. ACM Trans. Knowl. Discov. Data 14(5): 58:1-58:27 (2020)

51. Mingxing Duan, Kenli Li, Aijia Ouyang, Khin Nandar Win, Keqin Li, Qi Tian: EGroupNet: A Feature-enhanced Network for Age Estimation with Novel Age Group Schemes. ACM Trans. Multim. Comput. Commun. Appl. 16(2): 42:1-42:23 (2020)

52. Wangdong Yang, Kenli Li, Keqin Li: A Pipeline Computing Method of SpTV for Three-Order Tensors on CPU and GPU. ACM Trans. Knowl. Discov. Data 13(6): 63:1-63:27 (2019)

53. Xu Zhou, Kenli Li, ZhiBang Yang, Guoqing Xiao, Keqin Li: Progressive Approaches for Pareto Optimal Groups Computation. IEEE Trans. Knowl. Data Eng. 31(3): 521-534 (2019)

54. Jing Mei, Kenli Li, Zhao Tong, Qiang Li, Keqin Li: Profit Maximization for Cloud Brokers in Cloud Computing. IEEE Trans. Parallel Distributed Syst. 30(1): 190-203 (2019)

55. Yuedan Chen, Kenli Li, Wangdong Yang, Guoqing Xiao, Xianghui Xie, Tao Li: Performance-Aware Model for Sparse Matrix-Matrix Multiplication on the Sunway TaihuLight Supercomputer. IEEE Trans. Parallel Distributed Syst. 30(4): 923-938 (2019)

56. Jianguo Chen, Kenli Li, Kashif Bilal, Xu Zhou, Keqin Li, Philip S. Yu: A Bi-layered Parallel Training Architecture for Large-Scale Convolutional Neural Networks. IEEE Trans. Parallel Distributed Syst. 30(5): 965-976 (2019)

57. Z. Zhou, J. Qin, X. Xiang, Y. Tan, Q. Liu, et al., "News text topic clustering optimized method based on tf-idf algorithm on spark," Computers, Materials & Continua, vol. 62, no. 1, pp. 217–231, 2020.

58. J. Park and S. Kim, "Noise cancellation based on voice activity detection using spectral variation for speech recognition in smart home devices," Intelligent Automation & Soft Computing, vol. 26, no.1, pp. 149–159, 2020.

59. J. Deng, J. Chen and D. Wang, "Mechanism design and mechanical analysis of multi-suction sliding cleaning robot used in glass curtain wall," Computer Systems Science and Engineering, vol. 34, no.4, pp. 201–206, 2019.

60. X. Nie, X. Zou, and D. Zhu, "Modeling and simulation of entrepreneur individual based on dynamic and complex system computing," Computer Systems Science and Engineering, vol. 34, no.4, pp. 207–214, 2019.

61. Karimi, N., & Sarem, R. . (2021). Seismic response of multi-storey building using different vibration technique-A review. International Journal of Innovative Research and Scientific Studies, 4(1), 1–13. https://doi.org/10.53894/ijirss.v4i1.49

62. Ariffin, I. A., Ab Yajid, M. S., & Azam, S. F. An Analysis of the Construction Industry of Malaysia in view of the Dismissal Doctrine. Systematic Reviews in Pharmacy. 11(1), 834-842

63. Johar, M. G. M., Azam, S. F., & Ab Yajid, M. S. (2020). Information Mining Innovation and its Execution for an Information Digging Application in the Study of Deals Prescient. Systematic Reviews in Pharmacy, 11(1), 633-639.

64. Rahman, N., Othman, M., Yajid, M., Rahman, S., Yaakob, A., Masri, R., ... & Ibrahim, Z. J. M. S. L. (2018). Impact of strategic leadership on organizational performance, strategic orientation, and operational strategy. Management Science Letters, 8(12), 1387-1398.

65. Salam, A., Yaman, M. N., Hashim, R., Suhaimi, F. H., Zakaria, Z., & Mohamad, N. (2018). Analysis of Problems Posed in Problem Based Learning Cases: Nature, Sequence of Discloser and Connectivity with Learning Issues. Bangladesh Journal of Medical Science, 17(3), 417-423.

66. Vo, P. H., & Ngo, T. Q. (2021). The Role of Agricultural Financing and Development on Sustainability: Evidence from ASEAN Countries. AgBioForum, 23(1), 22-31.

67. Pinmongkhonkul, S., Khamkhunmuang, T., & Madhayamapurush, W. (2021). Ethnobotanical Study and Plant Dimension Classification in Kwan Phayao Community Areas, Phayao Province, Thailand. AgBioForum, 23(1), 65-71.

68. Navabian, M., Vazifehdost, M., Esmaeili Varaki, M. (2020). Estimation of pollution load to Anzali Wetland using remote sensing technique. Caspian Journal of Environmental Sciences, 18(3), 251-264. DOI: 10.22124/cjes.2020.4137

69. Khoshravan, H., Naqinezhad, A., Alinejad-Tabrizi, T., Yanina, T. (2019). Gorgan Bay environmental consequences due

to the Caspian Sea rapid water level change. Caspian Journal of Environmental Sciences, 17(3), 213-226. doi: 10.22124/cjes.2019.3664

70. Saleem, M. (2020). Microplane modeling of the elasto-viscoplastic constitution. Journal of Research in Science, Engineering and Technology, 8(3).

71. Aslanova, F. (2020). A comparative study of the hardness and force analysis methods used in truss optimization with metaheuristic algorithms and under dynamic loading. Journal of Research in Science, Engineering and Technology, 8(1), 25-33.

72. Akhir, E. A. P., Bachok, R., Arshad, N. I., & Zamri, A. A. (2018, August). Conceptual Framework for SIDS Alert System. In 2018 4th International Conference on Computer and Information Sciences (ICCOINS) (pp. 1-5). IEEE.

73. Jamal, A., Helmi, R. A. A., Syahirah, A. S. N., & Fatima, M. A. (2019, October). Blockchain-based identity verification system. In 2019 IEEE 9th International Conference on System Engineering and Technology (ICSET) (pp. 253-257). IEEE.

74. Davarpanah, A., Shirmohammadi, R., Mirshekari, B. and Aslani, A., 2019. Analysis of hydraulic fracturing techniques: hybrid fuzzy approaches. Arabian Journal of Geosciences, 12(13), pp.1-8.

75. Davarpanah, A. and Mirshekari, B., 2019. Mathematical modeling of injectivity damage with oil droplets in the waste-produced water re-injection of the linear flow. The European Physical Journal Plus, 134(4), p.180.

76. Valizadeh, K., Farahbakhsh, S., Bateni, A., Zargarian, A., Davarpanah, A., Alizadeh, A. and Zarei, M., 2020. A parametric study to simulate the non-Newtonian turbulent flow in spiral tubes. Energy Science & Engineering, 8(1), pp.134-149.

77. Zhu, G., Graham, D., Zheng, S., Hughes, J., and Greaves, D., 2020. Hydrodynamics of onshore oscillating water column devices: A numerical study using smoothed particle hydrodynamics. Ocean Engineering, 218, p.108226.

78. Karimi, N., & Sarem, R. . (2021). Seismic response of multi-storey building using different vibration technique-A review. International Journal of Innovative Research and Scientific Studies, 4(1), 1–13. https://doi.org/10.53894/ijirss.v4i1.49

79. Ariffin, I. A., Ab Yajid, M. S., & Azam, S. F. An Analysis of the Construction Industry of Malaysia in view of the Dismissal Doctrine. Systematic Reviews in Pharmacy. 11(1), 834-842

80. Johar, M. G. M., Azam, S. F., & Ab Yajid, M. S. (2020). Information Mining Innovation and its Execution for an Information Digging Application in the Study of Deals Prescient. Systematic Reviews in Pharmacy, 11(1), 633-639.

81. Rahman, N., Othman, M., Yajid, M., Rahman, S., Yaakob, A., Masri, R., ... & Ibrahim, Z. J. M. S. L. (2018). Impact of strategic leadership on organizational performance, strategic orientation, and operational strategy. Management Science Letters, 8(12), 1387-1398.

82. Salam, A., Yaman, M. N., Hashim, R., Suhaimi, F. H., Zakaria, Z., & Mohamad, N. (2018). Analysis of Problems Posed in Problem Based Learning Cases: Nature, Sequence of Discloser and Connectivity with Learning Issues. Bangladesh Journal of Medical Science, 17(3), 417-423.

83. Vo, P. H., & Ngo, T. Q. (2021). The Role of Agricultural Financing and Development on Sustainability: Evidence from ASEAN Countries. AgBioForum, 23(1), 22-31.

84. Pinmongkhonkul, S., Khamkhunmuang, T., & Madhayamapurush, W. (2021). Ethnobotanical Study and Plant Dimension Classification in Kwan Phayao Community Areas, Phayao Province, Thailand. AgBioForum, 23(1), 65-71.

85. Navabian, M., Vazifehdost, M., Esmaeili Varaki, M. (2020). Estimation of pollution load to Anzali Wetland using remote sensing technique. Caspian Journal of Environmental Sciences, 18(3), 251-264. doi: 10.22124/cjes.2020.4137

86. Khoshravan, H., Naqinezhad, A., Alinejad-Tabrizi, T., Yanina, T. (2019). Gorgan Bay environmental consequences due to the Caspian Sea rapid water level change. Caspian Journal of Environmental Sciences, 17(3), 213-226. doi: 10.22124/cjes.2019.3664

87. Saleem, M. (2020). Microplane modeling of the elasto-viscoplastic constitution. Journal of Research in Science, Engineering and Technology, 8(3).

88. Aslanova, F. (2020). A comparative study of the hardness and force analysis methods used in truss optimization with metaheuristic algorithms and under dynamic loading. Journal of Research in Science, Engineering and Technology, 8(1), 25-33.

89. Akhir, E. A. P., Bachok, R., Arshad, N. I., & Zamri, A. A. (2018, August). Conceptual Framework for SIDS Alert System. In 2018 4th International Conference on Computer and Information Sciences (ICCOINS) (pp. 1-5). IEEE.

90. Jamal, A., Helmi, R. A. A., Syahirah, A. S. N., & Fatima, M. A. (2019, October). Blockchain-based identity verification system. In 2019 IEEE 9th International Conference on System Engineering and Technology (ICSET) (pp. 253-257). IEEE.

91. https://doi.org/10.1016/j.renene.2022.08.121

92. https://doi.org/10.1016/j.ijmecsci.2021.106364

93. https://doi.org/10.1016/j.jsv.2021.116565